

Electrical characterization of p Ga As epilayers disordered by doped spin-on-glass

P. N. K. Deenapanray, M. Petracic, C. Jagadish, M. Krispin, and F. D. Auret

Citation: *Journal of Applied Physics* **97**, 033524 (2005); doi: 10.1063/1.1846140

View online: <http://dx.doi.org/10.1063/1.1846140>

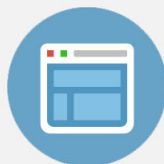
View Table of Contents: <http://scitation.aip.org/content/aip/journal/jap/97/3?ver=pdfcov>

Published by the [AIP Publishing](#)



Re-register for Table of Content Alerts

Create a profile.



Sign up today!



Electrical characterization of *p*-GaAs epilayers disordered by doped spin-on-glass

P. N. K. Deenapanray^{a)}

Centre for Sustainable Energy Systems, Department of Engineering, Faculty of Engineering and Information Technology, The Australian National University, Canberra, ACT 0200, Australia

M. Petracic and C. Jagadish

Department of Electronic Materials Engineering, Research School of Physical Sciences and Engineering, The Australian National University, Canberra, ACT 0200, Australia

M. Krispin

Lehrstuhl für Experimentalphysik IV, Institut für Physik, Universität Augsburg, 86135 Augsburg, Germany

F. D. Auret

Department of Physics, University of Pretoria, Pretoria 0002, South Africa

(Received 26 April 2004; accepted 9 November 2004; published online 19 January 2005)

Impurity-free disordering (IFD) of uniformly doped *p*-GaAs epitaxial layers was achieved using either undoped or doped (Ga or P) spin-on-glass (SOG) in conjunction with rapid thermal annealing in the temperature range from 800 to 925 °C. Capacitance-voltage measurements showed a pronounced increase in the doping concentration (N_A) in the near-surface region of the layers disordered using both undoped and P:SOG. The increase in N_A showed an Arrhenius-like dependence on the inverse of annealing temperature. On the other hand, N_A did not change significantly for Ga-doped SOG. These changes can be explained by the relative injection of excess gallium vacancies (V_{Ga}) during IFD of *p*-GaAs by the different SOG layers. Deep-level transient spectroscopy showed a corresponding increase in the concentration of a defect HA ($E_V+0.39$ eV), which can be attributed to Cu, in the undoped and P:SOG disordered *p*-GaAs layers, but not in the epilayers disordered by Ga:SOG. We have explained the increase in free carrier concentration by the segregation of Zn atoms towards the surface during the injection of V_{Ga} . The redistribution of Zn during disordering of buried marker layers in GaAs and $Al_{0.6}Ga_{0.4}As$ using either undoped or Ga-doped SOG was verified by secondary-ion mass spectrometry. © 2005 American Institute of Physics. [DOI: 10.1063/1.1846140]

I. INTRODUCTION

The monolithic integration of optoelectronic and photonic devices requires the selective area band-gap modification of III-V semiconductor compounds. One technique that has been widely investigated regarding its ability to achieve the band-gap engineering of III-V semiconductor heterostructures is impurity-free disordering (IFD).^{1,2} IFD uses dielectric capping layers that are deposited on the surface of the semiconductor structure and which, during a high-temperature annealing, have the ability to either increase or maintain the band gap of the structure. For instance, SiO_2 (Refs. 1–7) and SiO_xN_y (Ref. 2) capping layers can enhance disordering, whereas it can be suppressed by Si_3N_4 ,^{1,4} SrF_2 ,⁷ TiO_2 ,⁸ and gallium oxide⁹ layers. Spin-on-glass (SOG) capping layers are also attractive dielectrics for IFD since they are relatively cheap and do not require sophisticated equipment for their deposition. Further, their properties can be tailored by doping the SOG with different impurities.

It is generally accepted that in GaAs-based semiconductors, IFD is achieved by the injection of excess gallium vacancies (V_{Ga}) inside the material during the outdiffusion of Ga atoms into the dielectric capping layer at high

temperatures.^{1–9} Inhibiting IFD requires either suppressing the formation of V_{Ga} or preventing the diffusion of V_{Ga} into the bulk of the semiconductor once they are formed in the near-surface region of the semiconductor adjacent to the dielectric layer.^{4,6,8,9} In the light of this discussion, it can be said that IFD is a defect-driven process. Despite the fact that IFD is considered to be a simple process, it is masked by an underlying complex mechanism that is not well understood at present. The operative mechanism of IFD has remained elusive thus far because the apparently simple process is influenced by a myriad of interrelated factors, such as the type and quality of capping layer,^{1–3} stress,^{4,5,7–9} annealing ambient,⁴ and doping.¹⁰ In the past few years, we have devoted much research effort to understand the operative mechanism of IFD, leading us to study the defect reactions that drive the disordering process in *n*-type (Al) GaAs and *p*-type GaAs epilayers.¹¹ IFD of doped epilayers is of key interest from a device fabrication perspective since the migration of dopant atoms, such as Zn and Be, may cause the unwanted spatially nonselective impurity-induced disordering.^{12–15} Indeed, a recent study has demonstrated the adverse effects of Zn redistribution in IFD InGaAs/AlGaAs laser structures.¹⁰ Our previous studies have also demonstrated impurity relocation processes in IFD of *p*-type GaAs.¹¹ Since the vast majority of investigations of IFD

^{a)}Electronic mail: prakash.deenapanray@anu.edu.au

have focused on undoped device structures,^{1–9} we believe that there is a need to increase our understanding of impurity relocation processes in doped structures for practical reasons.

In this respect, we report on the influence of spin-on-glass doping on the creation of electrically active defects and impurity (Zn and Cu) segregation in IFD *p*-type GaAs epitaxial layers. The practical implications of atomic relocation processes in disordered *p*-GaAs are discussed in light of the application of the IFD process in device fabrication. However, this article does not attempt to resolve the contentious issues regarding the mechanism of impurity diffusion in disordered *p*-type GaAs.

II. EXPERIMENTAL PROCEDURE

Epitaxial GaAs (100) layers doped with $\sim 9 \times 10^{15}$ Zn/cm³ were grown by metalorganic chemical vapor deposition (MOCVD) at 750 °C. The epitaxial layers were spin-coated with undoped (U:SOG), P-doped (P:SOG), or Ga-doped (Ga:SOG) silicate SOG at 3000 rpm for 30 s. The samples were baked at 400 °C for 15 min before rapid thermal annealing (RTA) in the temperature range 800–925 °C for 30 s under Ar flow. The as-grown *p*-GaAs layers also received RTA in the same temperature range for control purposes. All samples were annealed using GaAs proximity capping. Following removal of the SOG layers, the GaAs layers were chemically cleaned prior to the fabrication of Ti Schottky barrier diodes, 200 nm thick and 0.77 mm in diameter. Ohmic contacts were made to the backside of samples using an In-Ga eutectic. High-frequency (1 MHz) capacitance-voltage (*C*-*V*), deep-level transient spectroscopy (DLTS) and photoluminescence (PL) measurements were used to characterize the disordered samples. The majority of DLTS measurements were made using a lock-in-type setup described in Ref. 16 in the 77–290 K temperature range, and DLTS depth profiling accounted for the “ λ -effect” using the methodology describe by Zohta and Watanabe.¹⁷ For DLTS measurements below 77 K, we used a lock-in amplifier in conjunction with a Boonton capacitance meter.¹⁸ PL measurements were performed using a 543.5 nm Ar-ion laser and a Si CCD detector with a built-in preamplifier via a 0.25 m spectrometer. The laser was shone on the sample through a chopper operating at a few hundred Hz.

The redistribution of Zn in GaAs and AlGaAs was also studied using secondary-ion mass spectrometry (SIMS). For this, 200-nm-wide buried Zn marker layers were grown by MOCVD in GaAs and Al_{0.6}Ga_{0.4}As epitaxial layers. These layers were spin-coated with either undoped or Ga-doped SOG followed by curing at 400 °C for 15 min. RTA was performed on the layers at 900 °C for 30 s under Ar flow, after which the dielectric layers were chemically removed. As-grown samples were annealed simultaneously for control purposes. All SIMS measurements were performed in a quadrupole-type ion microprobe (Riber MIQ 256) using 8-keV O₂⁺ sputtering at an angle of 45° with respect to the surface normal.

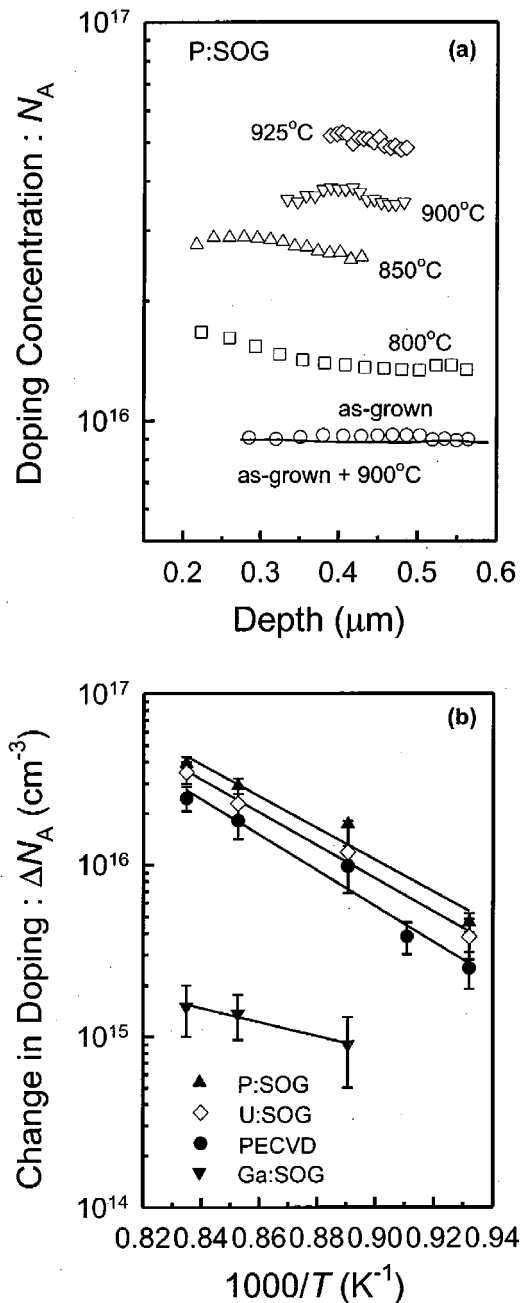


FIG. 1. (a) Doping profiles of *p*-GaAs disordered at different annealing temperatures using P:SOG. The solid line shows the concentration profiles for an as-grown sample annealed at 900 °C. The profiles were extracted from room temperature *C*-*V* measurements; and (b) the change in free carrier concentration, ΔN_A , for disordered sample relative to the as-grown sample at a depth of 0.4 μm .

III. RESULTS AND DISCUSSION

A. Doping concentration in disordered epilayers

Figure 1(a) illustrates the doping concentration (N_A) determined from *C*-*V* measurements at room temperature, in the as-grown (open circle) and disordered *p*-GaAs epilayers at different temperatures. In this example, IFD was achieved using P:SOG. The solid line shows the doping profile in an as-grown layer annealed at 900 °C for 30 s, which was typical for all annealing temperatures used in this study. Comparison between the solid line and data points shown by open circles reveals that annealing alone—i.e., without dielectric

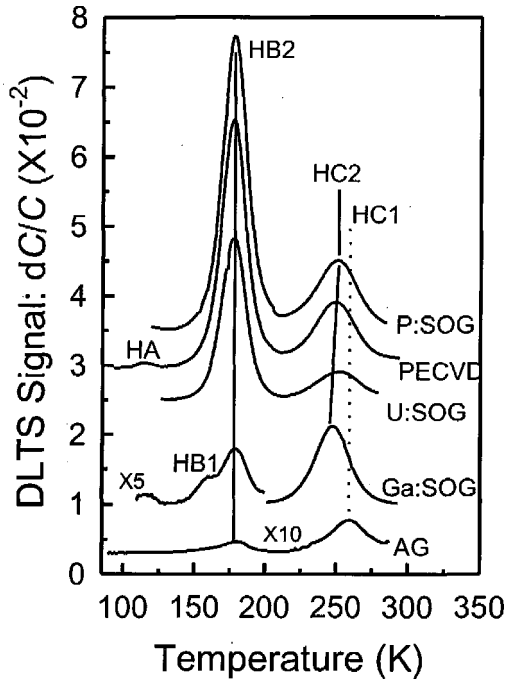


FIG. 2. DLTS spectra measured from as-grown and disordered *p*-GaAs samples. In each case, disordering was carried out at 900 °C for 30 s.

capping—did not change N_A in the present study. The disordered epilayers exhibit increased free carrier concentration in their near-surface regions (0.2–0.6 μm), with the effect becoming more pronounced at higher temperatures. The change in free carrier concentration, ΔN_A , for the different SOG layers is plotted in Fig. 1(b) as a function of the inverse of the annealing temperature. The value of ΔN_A corresponds to the difference between N_A in a dielectric-capped and annealed sample and N_A in the as-grown sample at a depth of 0.4 μm . We have previously measured the changes in N_A for samples disordered using plasma-enhanced chemical vapor deposited (PECVD) SiO_2 ,¹⁹ and the results (solid circles) are also shown in Fig. 1(b). There is an Arrhenius-like dependence of ΔN_A on $1/T$ for U:SOG, P:SOG, and PECVD SiO_2 with an activation energy in the range 1.9–2.1 eV. The similar activation energy suggests that the same mechanism is responsible for the increase in N_A from these three different dielectric layers. On the other hand, ΔN_A remained unchanged, within the experimental error, for samples capped with Ga:SOG. A change in N_A can be explained by either (1) the segregation of Zn dopant atoms, and/or (2) an increase in acceptor-type defects in the near-surface region of the disordered samples. These mechanisms are suppressed in the case of Ga:SOG. In order to understand the relative contribution of the two mechanisms on the change in free carrier concentration, we have performed DLTS measurements of the electrically active defects in the disordered layers. Since the uncapped and annealed samples did not exhibit any change in doping concentration compared to the as-grown samples, we can safely exclude purely thermal effects as the cause for the changes in N_A .

B. Deep-level transient spectroscopy measurements

The DLTS spectra shown in Fig. 2 were measured from

the as-grown epilayer and samples disordered using various SOG layers or PECVD SiO_2 at 900 °C for 30 s. By varying the bias conditions, the region extending between ~ 0.43 and ~ 0.57 μm was probed by DLTS. Arrhenius plots of $\ln(T^2/e_h)$ versus $1000/T$ were used to determine the activation energy (E_T) and apparent capture cross section (σ_a) of defects (i.e., “signature”). These plots are not shown here because they are identical to those we have reported previously.¹⁹ We also compared the signatures of IFD-induced defects in *p*-GaAs with those reported in the literature in order to allow their tentative identification. The as-grown layers contained the defects commonly observed in MOCVD-grown *p*-GaAs: HB2 ($E_T \sim E_V + 0.39$ eV; $\sigma_a \sim 6.3 \times 10^{-15}$ cm^2) and HC1 ($E_T \sim E_V + 0.57$ eV; $\sigma_a \sim 3.0 \times 10^{-15}$ cm^2), in concentrations $\sim 2 \times 10^{12}$ and $\sim 4 \times 10^{12}$ cm^{-3} , respectively. Based on the report by Mitonneau *et al.*,²⁰ we identified HB2 and HC1 to Cu (HL4)- and Fe-related (HL3) defects, respectively. The disordered samples contain a defect HC2 ($E_T \sim E_V + 0.55$ eV; $\sigma_a \sim 2.7 \times 10^{-15}$ cm^2) which has a lower-temperature peak position than HC1. However, the extent of the peak shift appears to depend on the type of capping layer used (i.e., ~ 11 K for Ga:SOG and ~ 8 K for P:SOG). This suggests that the defect peak at ~ 250 K in the DLTS spectra of disordered samples may consist of the superposition of HC1 and HC2.²¹ Following our present understanding of IFD in GaAs,^{11,19} we speculate that HC2 may be a defect related to either the As_i (H3)²² or As_{Ga} (HM1).²³ One qualification to this tentative assignment is that the double donor state of EL2 [i.e., $\text{HM1}-\text{As}_{\text{Ga}}(+/+)$] has not previously been observed in epitaxially grown *p*-GaAs layers. We have previously attributed HA and HB1,¹⁹ which are of minor interest here, to defect complexes involving Zn (Ref. 20) and Cu,²² respectively.

A more pertinent observation concerning the present study is the higher intensity of HB2 in the disordered samples (discounting Ga:SOG). As mentioned earlier, we have previously attributed HB2 to the Cu-related acceptor level in *p*-GaAs, but without providing much evidence for the assignment.¹⁹ Before discussing the effect of annealing temperature on the creation of this prominent defect in disordered *p*-GaAs, we discuss the electrical and optical properties of HB2 in more detail. It is well established that Cu introduces two acceptor levels at $E_V + (0.13\text{--}0.15)$ eV and $E_V + (0.40\text{--}0.49)$ eV in the band gap of GaAs, albeit the exact structure of these levels are not known.^{20,24–26} It is often speculated that the two defects are two different charge states of the double acceptor Cu_{Ga} , but other defect structures involving complexes of Cu_{Ga} and V_{As} (arsenic vacancy) could also be possible candidates.²⁵ The DLTS spectrum shown in Fig. 3(a) was measured from a sample disordered using PECVD SiO_2 at 900 °C for 30 s. It depicts two prominent levels at $E_V + 0.13$ eV and $E_V + 0.49$ eV, which correspond remarkably well with those expected for the two Cu-related acceptor levels in *p*-GaAs. Furthermore, the PL spectrum measured from the same sample illustrates the presence of a peak at 1.36 eV (see inset), as shown in Fig. 3(b).^{23,24} This peak is due to a donor-acceptor pair recombination involving the Cu-related level $E_V + 0.13$ eV. We believe that the com-

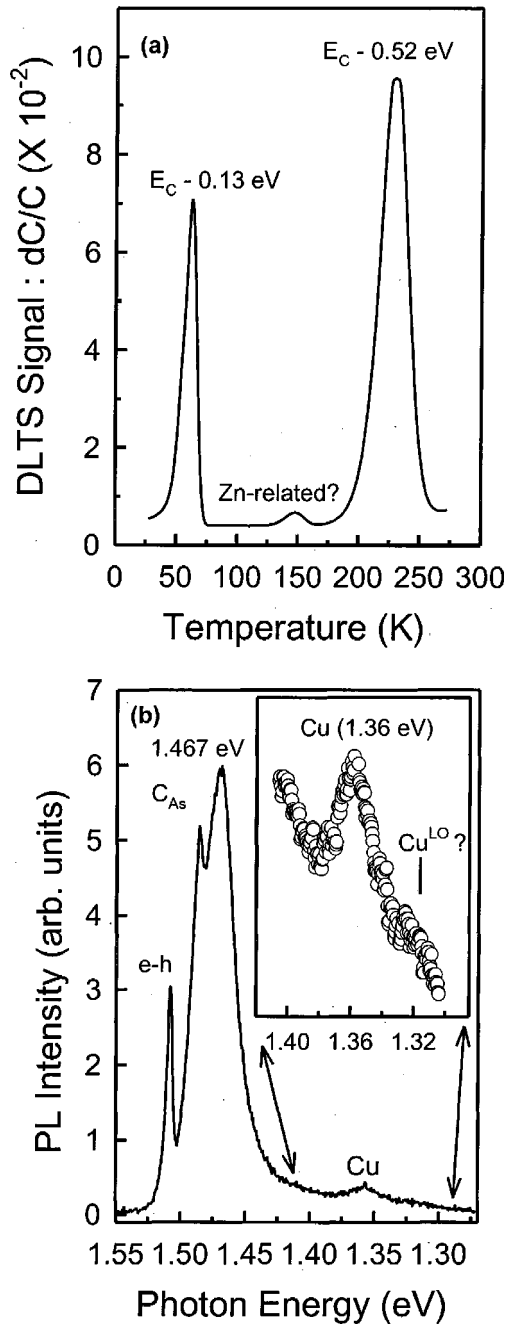


FIG. 3. (a) DLTS spectrum depicting two prominent levels at $E_V+0.13$ eV and $E_V+0.49$ eV, which correspond to the two Cu-related acceptor levels in p -GaAs, and (b) PL spectra which demonstrate the presence of the 1.36 eV transition between a donor and the Cu-related $E_V+0.13$ eV acceptor level. The spectra were measured from a sample disordered using PECVD SiO_2 at 900 °C for 30 s.

bination of low-temperature DLTS and PL results shown in Fig. 3 provides the evidence for relating HB2 to Cu.

Having established that the prominent defect HB2 is an acceptor-type level, its concentration in disordered samples should influence ΔN_A shown in Fig. 1(b). Hence, we now turn to the annealing temperature dependence of the creation of HB2. Figure 4(a) illustrates the Arrhenius-like dependence of the peak intensity ($\Delta dC/C$) of HB2 on the inverse of annealing temperature for the four capping layers. The right axis of Fig. 4(a) shows the defect concentration (N_T) based on the approximation that $N_T \sim 2(\Delta dC/C)N_A$, where N_A was

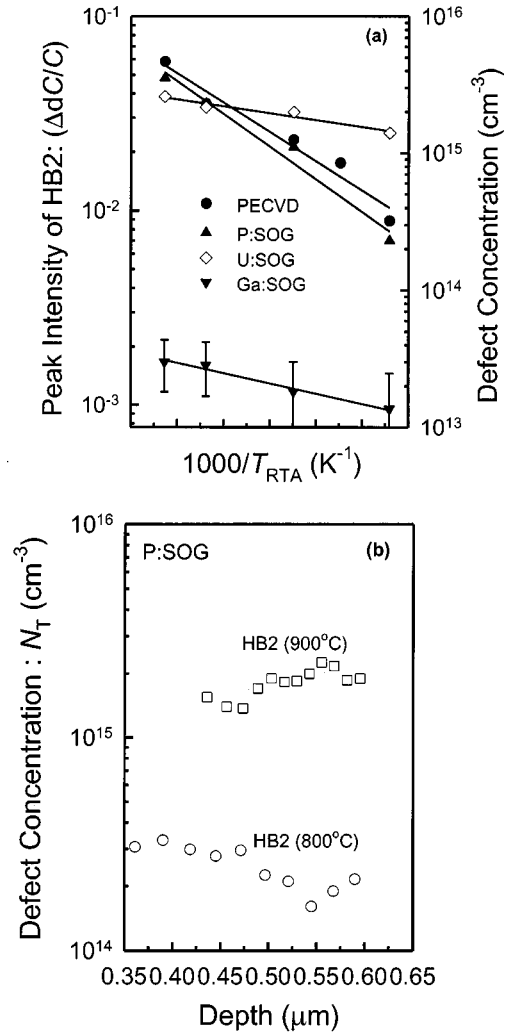


FIG. 4. (a) Arrhenius-like dependence of the peak intensity and concentration of HB2 in disordered samples. (b) Selected DLTS depth profile of HB2 in p -GaAs disordered at 800 °C (open circles) or 900 °C using P:SOG. The uniform distribution of HB2 was typical for other capping layers.

determined from C - V measurements at ~ 177 K. The selected DLTS depth profiles of HB2 in p -GaAs disordered using P:SOG in Fig. 4(b) shows that it has a fairly uniform distribution. The depth distribution of HB2 was similarly uniform in samples disordered using other capping layers, over the entire temperature range studied here. The concentration profiles of HB2 in Fig. 4(b) demonstrate that the approximation used above to convert the peak intensity of HB2 into an equivalent defect concentration in Fig. 4(a) is valid. The results shown in Fig. 4(a) are similar to those depicted in Fig. 1(b) in that they also exhibit an Arrhenius-like dependence on the inverse of annealing temperature. However, one exception to this behavior is the case of U:SOG, which gives an almost temperature-independent introduction of HB2.

We now discuss the influence of disordering on the concentration of Cu (i.e., HB2). First, a note is made regarding the source of Cu in our samples. The high purity gases and organometallic sources used in our MOCVD growth preclude the incorporation of Cu in the epitaxial layers from the vapor phase. PL measurements have revealed (not shown) that the concentration of Cu in the p^+ -substrate was at least

one order of magnitude higher than in the disordered epilayers. Here, we may confidently say that the Cu observed in epilayers originates from the p^+ -substrates in which they are grown. The diffusion of Cu ($\sim 4 \times 10^{12} \text{ cm}^{-3}$ of HB2 in the as-grown sample) into the epilayers occurs already during growth at 750°C . Cu diffuses rapidly in GaAs even at low temperatures, presumably as an interstitial species (Cu_i), whereas substitutional Cu (Cu_{Ga}) is relatively immobile.^{26–28} There are two mechanisms that result in the formation of Cu_{Ga} , and they only differ in the way by which Cu is substituted on the Ga sublattice. The kick-out process requires the presence of Ga_i (i.e., $\text{Cu}_i + \text{Ga}_{\text{Ga}} \rightarrow \text{Cu}_{\text{Ga}} + \text{Ga}_i$), whereas the substitutional (or interstitial-substitutional) process involves V_{Ga} (i.e., $\text{Cu}_i + \text{V}_{\text{Ga}} \rightarrow \text{Cu}_{\text{Ga}}$). Although the kick-out mechanism is the favored model for the diffusion of Cu, our results suggest that the vacancy-assisted process becomes dominant under the nonequilibrium injection of V_{Ga} during IFD using U:SOG, P:SOG, or PECVD.^{11,19} In a previous study, we have shown that the segregation of Cu was much lower in samples disordered using anodic oxides of GaAs rather than PECVD SiO_2 .²⁹ The reason for this was the lower concentration of excess V_{Ga} produced during disordering by native oxides compared to SiO_2 . Furthermore, the tendency of Cu to decorate open volume defects in GaAs (i.e., voids)²⁸ implies that the injection of excess V_{Ga} may well provide the driving force for the segregation of Cu towards the surface. Since the original concentration of Ga in Ga:SOG is higher than the concentration of Ga atoms that a U:SOG layer can accommodate during annealing, the creation of V_{Ga} , and hence HB2, is suppressed during IFD of p -GaAs using Ga:SOG. The concentration of Ga in doped and undoped SOG layers was measured by in-depth x-ray photoelectron spectroscopy profiling in Ref. 30. It is worth noting here that previous studies have reported that the diffusion of Cu in GaAs-created defects. For instance, Leon *et al.*²⁶ have reported on electrically inactive Cu in the form of Cu-Ga precipitates, while Hutchinson and Ball³¹ reported large increases in perfect and faulted loops in Cu-diffused semi-insulating and Si-doped GaAs, respectively. The concentrations of Cu in our disordered samples are twenty times below the solid solubility of Cu in GaAs.^{26,27} We do not expect these low concentrations of Cu to create defects in our samples.

We are now in a position to discuss the changes in N_A shown in Fig. 1. It is clear from Fig. 4(a) that the concentration of the HB2 (acceptor-type deep level) cannot account for the increase in the free carrier concentration in the near-surface region of IFD p -GaAs samples. In fact, except for the concentration of HB2 obtained by disordering with U:SOG at 800°C (i.e., $1000/T_{\text{RTA}} = 0.93 \text{ K}^{-1}$), the defect concentrations in Fig. 4(a) are one order magnitude lower than ΔN_A [Fig. 1(b)]. This conclusion remains unchanged even if the Cu-related levels in Fig. 3(a) were related to the Cu_{Ga} double acceptor. We therefore arrive at the conclusion that the pronounced increase in the doping concentration in the near-surface region of disordered p -GaAs epilayers is mostly due to the relocation of Zn. The segregated Zn in the top $\sim 0.5 \mu\text{m}$ layer could come from the underlying epilayer

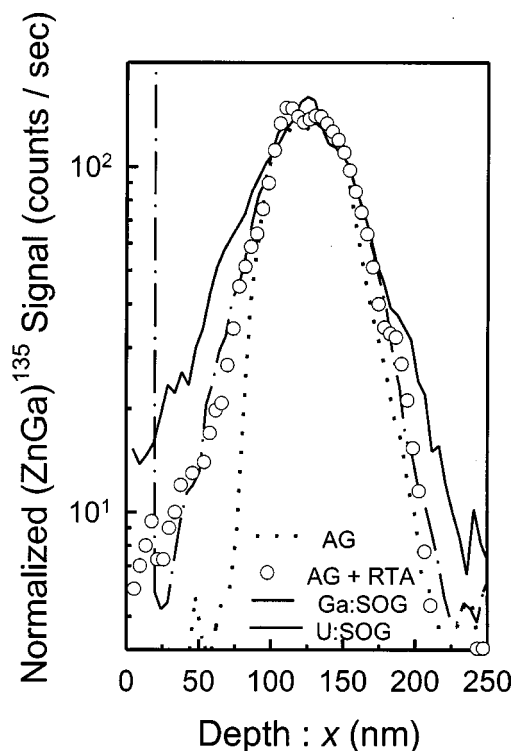


FIG. 5. SIMS in-depth profile of a Zn buried marker layer in GaAs using either U:SOG or uncapped and annealed layer is shown in open circle. Disorderer was carried out at 900°C for 30 s.

and/or the p^+ -substrate. The evidence for such a claim can be verified by SIMS analysis, which is discussed next.

C. SIMS analysis

Since the concentration of Zn in disordered p -GaAs samples is below the detection limit of our instrument, we have performed SIMS analysis of Zn diffusion in buried marker layers of Zn in both GaAs and AlGaAs. In order to demonstrate the effect of Zn relocation, we have used only U:SOG and Ga:SOG capping layers. The Zn in-depth profiles shown in Figs. 5 and 6 for IFD GaAs and $\text{Al}_{0.6}\text{Ga}_{0.4}\text{As}$, respectively, are qualitatively similar. The as-grown buried Zn marker layers have sharpest profiles (dotted lines). In GaAs, annealing only broadens the Zn profiles (open circles) because of the presence of a concentration gradient. A comparison between the profiles shown in dashed lines and open circles in Fig. 5 demonstrates that disordering by Ga:SOG produces the same effect on Zn as in the as-grown and annealed case. This effect is similar to that shown in Fig. 1(b), where it was shown that the free carrier concentration did not change following disordering by Ga:SOG. However, the same cannot be said for annealing under Ga:SOG in $\text{Al}_{0.6}\text{Ga}_{0.4}\text{As}$. In this case, the profile broadening, especially for Al, is larger compared for the profiles from the uncapped and annealed sample. In both cases, the U:SOG layer produces the highest disordering, that is largest redistribution of Zn and Al, with a net asymmetry in the broadened profiles towards the surface; i.e., relative to the profiles from as-grown samples.

The results shown in Figs. 5 and 6 are similar to the investigation of the evolution of a Be (similar diffusion be-

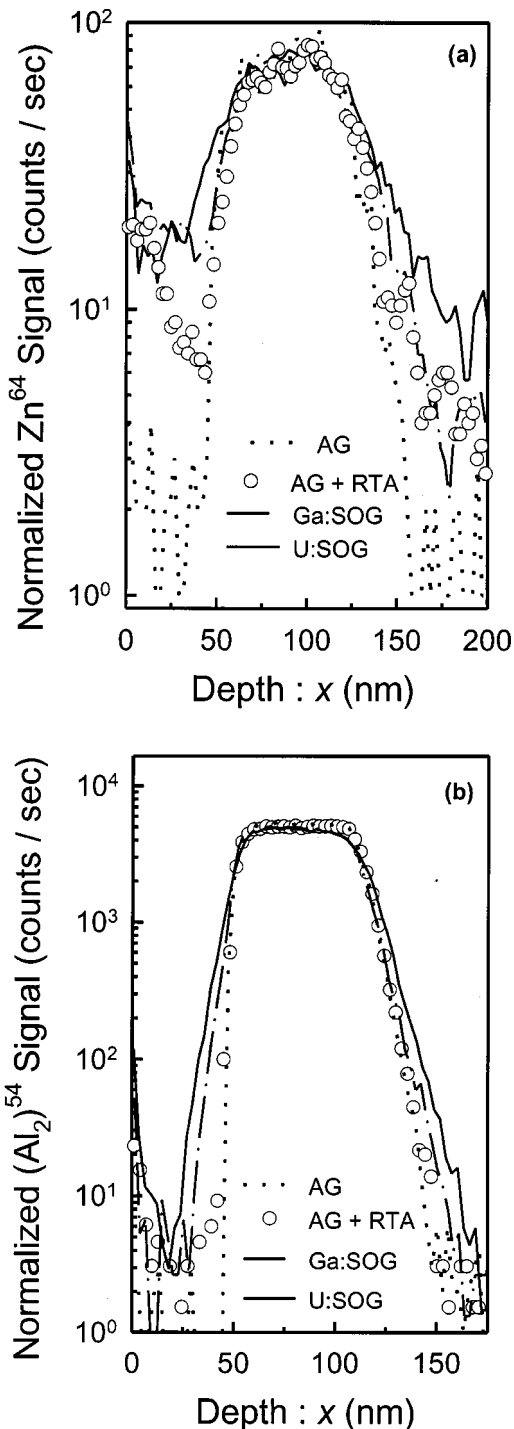


FIG. 6. SIMS in-depth profiles of (a) Zn and (b) Al from a Zn buried marker layer grown in $\text{Al}_{0.6}\text{Ga}_{0.4}\text{As}$ using either Ga:SOG or U:SOG. Disorder was carried out at 900°C for 30 s.

havior as Zn)^{6,12} marker in GaAs during IFD using SiO_2 and Si_3N_4 capping layers.¹⁵ In that study, Haddara *et al.*¹⁵ concluded that the redistribution of Be involved time-dependent concentrations of both V_{Ga} and Ga_i . Accordingly, the SIMS profile broadening reported here can be explained by looking at the interaction between these two species. In the uncapped and Ga:SOG-capped and annealed GaAs sample, broadening relative to the as-grown sample proceeds by the kick-out mechanism that is mediated by Ga_i^{2+} ,^{6,12-14} Under the non-equilibrium injection of V_{Ga} (or V_{Ga}^{3-}); i.e., annealing under

U:SOG capping, interstitial gallium is annihilated, and the excess of vacancies enhance Zn profile broadening according to the I-S mechanism. Since the diffusion length of V_{Ga} in GaAs is short,^{32,33} the flux of vacancies can be expected to decrease with distance below the surface. Hence, the concentration of V_{Ga} intersecting the rising edge of the Zn profile can be expected to be larger than the concentration intersecting the falling edge of the profile. This produces an asymmetric broadening of the Zn profile towards the surface. This depth dependence of the flux of vacancies also explains the similar asymmetry for Zn and Al profiles obtained in disordered $\text{Al}_{0.6}\text{Ga}_{0.4}\text{As}$ by U:SOG. The larger interdiffusion of Al and An in Ga:SOG disordered $\text{Al}_{0.6}\text{Ga}_{0.4}\text{Ag}$ compared to the uncapped and annealed sample is ambiguous. However, it does reveal that there is an enhancement of group III interstitials during disordering by Ga:SOG, which would be similar to the enhanced interdiffusion of a Be marker layer disordered by Si_3N_4 capping.¹⁵ Since the only difference between our two structures is the presence (or absence) of Al, the results in Fig. 6 suggest that there may be an oversaturation of aluminum interstitials at the interfaces during annealing by Ga:SOG. This oversaturation effect may proceed by a mechanism similar to the swapping between interstitial Zn and substitutional Be.³⁴ The swapping between interstitial zinc and substitutional Al is favorable because Zn has an atomic radius that more closely matches that of Ga. At this stage, this effect remains unclear to us. It suffices to mention here that the disordering of Zn and Al buried marker layers is a subject of our ongoing research.

The main point to retain from this discussion is the clear process of V_{Ga} -enhanced disordering. Although there is no overwhelming evidence for the exact mechanism that is responsible for Zn diffusion in GaAs, the kick-out mechanism is the generally accepted model (similar to Cu and Be).^{6,12-14} As our results demonstrate, it is very difficult to maintain this model under IFD conditions producing a nonequilibrium concentration of V_{Ga} . This conclusion is consistent with those of Ky *et al.*,¹³ who have shown that V_{Ga} played an important role in the diffusion of Zn in GaAs doped as low as $\sim 4 \times 10^{16}$ Zn/cm³ under equilibrium condition. The results reported here show that both Cu and Zn diffuse towards the near-surface of disordered *p*-GaAs epilayers where an excess of V_{Ga} is injected; that is, for U:SOG, P:SOG, and PECVD SiO_2 . The similar changes in free carrier concentration in *p*-GaAs following disordering using U:SOG, P:SOG, and PECVD SiO_2 suggest that the concentration of excess V_{Ga} created by these capping layers is similar. However, the reason for the temperature dependence of HB2 when U:SOG is used is not clear to us at the present time. Since the generation of V_{Ga} is suppressed when Ga:SOG is used, the redistribution of Zn and Cu (HB2) are minimal. It is worth noting here that we do not expect zinc precipitates to form in the lowly-doped epilayers ($< 5 \times 10^{16}$ Zn cm⁻³) used here. Such defects have previously been observed only in heavily Zn-diffused samples.^{31,35,36} We cannot exclude the formation of such defects in the heavily doped Zn-marker samples. These are currently being investigated as mentioned earlier. It is pointed out here that the SIMS results are used merely to

support our claim that the diffusion of Zn is enhanced under disordering conditions that produce an excess V_{Ga} .

In light of the results reported here, further research is required to find capping layers and/or experimental conditions that may produce the sufficient disordering required for device integration, while minimizing the segregation of fast impurities. Impurity diffusion leads to the uncontrollable impurity-induced disordering that is detrimental for practical purposes. We have recently demonstrated that an anodic oxide of Ga and As is a promising candidate for a capping layer that minimizes the atomic relocation of Zn and Cu.²⁹ However, the practical application of such a capping layer in device integration remains to be demonstrated. Alternatively, the use of carbon as a *p*-type dopant should receive more research focus.

IV. CONCLUSION

In summary, we have used capacitance-voltage, deep-level transient spectroscopy, photoluminescence, and secondary-ion mass spectrometry techniques to characterize impurity-free disordering of *p*-GaAs epitaxial layers using doped and undoped spin-on-glasses. Samples disordered using U:SOG, P:SOG, or PECVD SiO₂ exhibited a pronounced increase in doping concentration N_A in their near-surface region, whereas this effect was minimized for Ga:SOG. We have demonstrated that the change in free carrier concentration could not be explained only by the creation of acceptor-type defects related to Cu. An explanation of the increase in N_A needs to consider the segregation of Zn atoms towards the surface of the disordered samples. We have explained the changes in N_A can be explained by the relative injection of nonequilibrium concentrations of gallium vacancies (V_{Ga}) during IFD of *p*-GaAs by the different SOG layers, which in the cases of U:SOG, P:SOG, and PECVD SiO₂ cause Cu and Zn impurities to relocate towards the surface of samples. The redistribution of Zn during disordering of buried marker layers in GaAs and Al_{0.6}Ga_{0.4}As using either undoped or Ga-doped SOG was verified by secondary-ion mass spectrometry. This strong impurity relocation process poses additional constraints on the application of IFD in the integration of optoelectronic devices that are doped with fast diffusers such as Zn or Be. We have also discussed the practical implications of the redistribution of fast diffusers during IFD as far as its application to device fabrication is concerned.

ACKNOWLEDGMENT

One of the authors (P. N. K. D.) acknowledges the financial support of the Australian Research Council. A second (F. D. A.) is grateful to the National Research Foundation, South Africa, for its financial support.

¹D. G. Deppe, L. J. Guido, N. Holonyak, Jr., K. C. Hsieh, R. D. Burnham, R. L. Thornton, and T. L. Paoli, *Appl. Phys. Lett.* **49**, 510 (1986).

- ²S. Bürkner, M. Maier, E. C. Larkins, W. Rothmund, E. P. O'Reilly, and J. D. Ralston, *J. Electron. Mater.* **24**, 805 (1995).
- ³P. N. K. Deenapanray, L. Fu, H. H. Tan, and C. Jagadish, *Electrochem. Solid-State Lett.* **3**, 196 (2000); P. N. K. Deenapanray and C. Jagadish, *J. Vac. Sci. Technol. B* **19**, 1962 (2001).
- ⁴A. Pépin, C. Vieu, M. Schneider, H. Launois, and Y. Nissim, *J. Vac. Sci. Technol. B* **15**, 142 (1997).
- ⁵P. N. K. Deenapanray and C. Jagadish, *Electrochem. Solid-State Lett.* **4**, G11 (2001).
- ⁶R. M. Cohen, *Mater. Sci. Eng., R.* **20**, 167 (1997).
- ⁷B. S. Ooi, K. McIlvaney, M. W. Steet, A. Saher Helmy, S. G. Ayling, A. C. Bryce, J. H. Marsh, and J. S. Roberts, *IEEE J. Quantum Electron.* **33**, 1784 (1997).
- ⁸L. Fu, P. Lever, H. H. Tan, C. Jagadish, P. Reece, and M. Gal, *Appl. Phys. Lett.* **82**, 2613 (2003).
- ⁹L. Fu, J. Wong-Leung, P. N. K. Deenapanray, H. H. Tan, C. Jagadish, B. Gong, R. N. Lamb, R. M. Cohen, W. Reichert, L. V. Dao, and M. Gal, *J. Appl. Phys.* **92**, 3579 (2002).
- ¹⁰M. Buda, J. Hay, H. H. Tan, L. Fu, C. Jagadish, P. Reece, and M. Gal, *J. Electrochem. Soc.* **150**, G481 (2003).
- ¹¹P. N. K. Deenapanray, M. Krispin, W. E. Meyer, H. H. Tan, C. Jagadish, and F. D. Auret, *Mater. Res. Soc. Symp. Proc.* **799**, 103 (2004).
- ¹²S. Yu, T. Y. Tan, and U. Gösele, *J. Appl. Phys.* **69**, 3547 (1991).
- ¹³N. H. Ky, L. Pavesi, D. Araujo, J. D. Ganiere, and F. K. Reinhart, *J. Appl. Phys.* **69**, 7585 (1991).
- ¹⁴D. G. Deppe and N. Holonyak, Jr., *J. Appl. Phys.* **64**, R93 (1989).
- ¹⁵Y. M. Haddara, M. D. Deal, and J. C. Bravman, *Appl. Phys. Lett.* **68**, 1939 (1996).
- ¹⁶B. G. Svensson, K.-H. Rydén, and B. M. S. Lewerentz, *J. Appl. Phys.* **66**, 699 (1989).
- ¹⁷Y. Zohta and M. O. Watanabe, *J. Appl. Phys.* **53**, 1809 (1982).
- ¹⁸F. D. Auret, *Rev. Sci. Instrum.* **57**, 1597 (1986).
- ¹⁹P. N. K. Deenapanray, A. Martin, S. Doshi, H. H. Tan, and C. Jagadish, *Appl. Phys. Lett.* **81**, 3573 (2002).
- ²⁰A. Mitonneau, G. M. Martin, and A. Mircea, *Electron. Lett.* **13**, 666 (1977).
- ²¹The relative concentrations of HC1 and HC2, depending on the type of capping layer, produce different peak positions of HC2 relative to that of HC1. A larger difference between the peak positions of HC1 and HC2 would imply a larger contribution from HC1, and vice versa.
- ²²D. Stevenard, X. Boddaert, and J. C. Bourgoin, *Phys. Rev. B* **34**, 4048 (1986).
- ²³J. Lagowski, D. G. Lin, T.-P. Chen, M. Skowronski, and H. C. Gatos, *Appl. Phys. Lett.* **47**, 929 (1985).
- ²⁴G. Hofmann, J. Madok, N. M. Naegel, G. Roos, N. M. Johnson, and E. E. Haller, *Appl. Phys. Lett.* **61**, 2914 (1992).
- ²⁵Z. G. Wang, H. P. Gislason, and B. Monemar, *J. Appl. Phys.* **58**, 230 (1985).
- ²⁶R. Leon, P. Werner, K. M. Yu, M. Kaminska, and E. R. Weber, *Appl. Phys. A: Mater. Sci. Process.* **61**, 7 (1995).
- ²⁷R. N. Hall and J. H. Racette, *J. Appl. Phys.* **35**, 379 (1964).
- ²⁸R. Krause-Rehberg, K. Petters, and J. Gebauer, *Physica B* **273–274**, 714 (1999).
- ²⁹*G37* (2003)
- ³⁰P. N. K. Deenapanray, B. Gong, R. N. Lamb, A. Martin, L. Fu, H. H. Tan, and C. Jagadish, *Appl. Phys. Lett.* **80**, 4351 (2002).
- ³¹P. W. Hutchinson and R. K. Ball, *J. Mater. Sci.* **17**, 406 (1982).
- ³²K. Wittmack, *Vacuum* **34**, 119 (1984).
- ³³P. J. Poole, S. Charbonneau, G. C. Aers, T. E. Jackman, M. Buchanan, M. Dion, R. D. Goldberg, and I. V. Mitchell, *J. Appl. Phys.* **78**, 2367 (1995).
- ³⁴P. A. Houston, F. R. Shepherd, A. J. SpringThorpe, P. Mandeville, and A. Margittai, *Appl. Phys. Lett.* **52**, 1219 (1988).
- ³⁵M. Luysberg, W. Jäger, K. Urban, M. Schänzer, N. A. Stolwijk, and H. Mehrer, *Mater. Sci. Eng., B* **13**, 137 (1992).
- ³⁶Y. C. Lu, T. S. Kalkur, and C. A. Paz de Araujo, *J. Electron. Mater.* **19**, 29 (1990).